Hindawi
Advances in Condensed Matter Physics
Volume 2017, Article ID 3836204, 5 pages
https://doi.org/10.1155/2017/3836204

Research Article

Absorption Spectrum and Density of States of Square, Rectangular, and Triangular Frenkel Exciton Systems with Gaussian Diagonal Disorder

Ibrahim Avgin[1] and David Huber[2]

[1]*Department of Electrical and Electronic Engineering, Ege University, Bornova, 3500 Izmir, Turkey*
[2]*Physics Department, University of Wisconsin-Madison, Madison, WI 53706, USA*

Correspondence should be addressed to David Huber; dhuber@wisc.edu

Received 17 March 2017; Revised 10 July 2017; Accepted 16 July 2017; Published 14 August 2017

Academic Editor: Oleg Derzhko

Using the coherent potential approximation, we investigate the effects of disorder on the optical absorption and the density of states of Frenkel exciton systems on square, rectangular, and triangular lattices with nearest-neighbor interactions and a Gaussian distribution of transition energies. The analysis is based on an elliptic integral approach that gives results over the entire spectrum. The results for the square lattice are in good agreement with the finite-array calculations of Schreiber and Toyozawa. Our findings suggest that the coherent potential approximation can be useful in interpreting the optical properties of two-dimensional systems with dominant nearest-neighbor interactions and Gaussian diagonal disorder provided the optically active states are Frenkel excitons.

1. Introduction

In a series of recent papers [1–3], we have applied the coherent potential approximation (CPA) to the calculation of the optical absorption and density of states of the Frenkel exciton model in one- and three-dimensional arrays with nearest-neighbor interactions and Gaussian disorder associated with the single-site transition energies. In the case of the one-dimensional systems we have shown that the results for the density of states are in excellent agreement with numerical calculations carried out on arrays of 10^7–10^8 sites [1]. The accuracy of the CPA for the optical absorption in one dimension [2] was tested in a comparison with data obtained from finite-array calculations by Schreiber [4]. Good agreement was obtained with the ensemble average of data from arrays of 199 sites. The CPA was applied to cubic lattices in [3]. In the case of the simple cubic lattice, good agreement was obtained with the corresponding finite-array calculations of Schreiber and Toyozawa [5, 6] for the optical absorption and the density of states. Along with the simple cubic data, corresponding CPA results were reported for the body-centered and face-centered cubic lattices.

A preliminary CPA analysis of the optical absorption and the density of states for the square lattice was reported in [7]. The approach followed was based on a large-energy expansion of Green's function, and the calculations were limited to energies below the absorption edge of the ideal system. Like the simple cubic analysis, the results were in good agreement with findings reported in [5, 6]. In this paper, we investigate the square lattice using an approach for the calculation of Green's function that is based on the evaluation of a complete elliptic integral of the first kind. Unlike the previous approach, we obtain results that are applicable over the entire absorption band. We also extend the theory to rectangular and triangular lattices for which there are no finite-array results to compare with.

In the CPA, the starting point in all three dimensions is lattice Green's function, $G_0(E)$, which in turn depends on

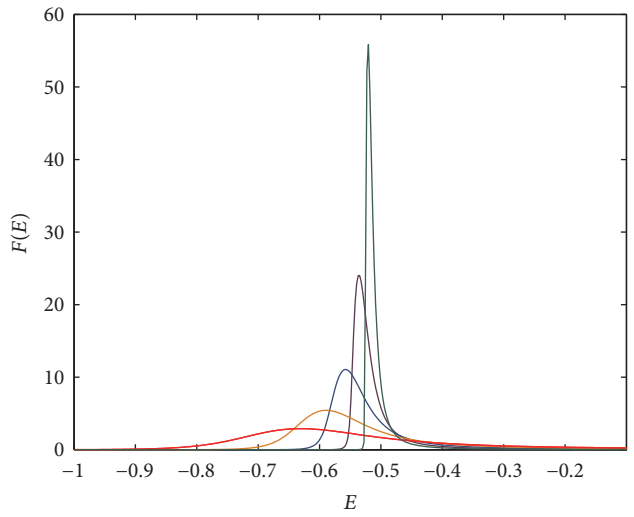

FIGURE 1: Normalized optical absorption for the square lattice. From left to right along the energy axis, the curves correspond to $\sigma = 0.263$, 0.186, 0.131, 0.093, and 0.066. In this and all other figures, energy is in units of the band width.

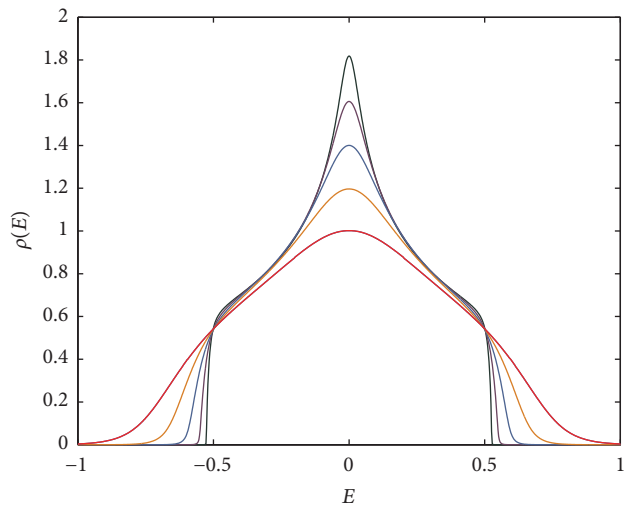

FIGURE 2: Normalized density of states for the square lattice. From left to right along the energy axis, the curves correspond to $\sigma = 0.263$, 0.186, 0.131, 0.093, and 0.066.

the structure of the lattice. The calculation of the optical absorption and the density of states follow once one knows CPA Green's function which is obtained from lattice Green's function by the replacement $E \to E - V_C(E)$, where $V_C(E)$ is the coherent potential. Equations relating to the calculation of $V_C(E)$ and the connection of CPA Green's function to the absorption and the density of states are given in [1–3] and will not be reproduced here.

2. Square Lattice

In analyzing the square, rectangular, and triangular systems, we take the unit of energy to be the width of the ideal (no disorder) exciton band and assume the absorption edge is at the bottom of the band. In the case of the square lattice, this leads to the exciton energy

$$E_{\mathbf{k}} = -\left(\frac{1}{4}\right)\left(\cos k_x + \cos k_y\right) \tag{1}$$

in the absence of disorder. The corresponding expression for ideal Green's function for complex energy takes the form [8]

$$G_0(E) = \left(\frac{2}{\pi E}\right)\mathbf{K}\left(2E^{-1}\right), \tag{2}$$

where $\mathbf{K}(m)$ denotes the complete elliptic integral with modulus m.

The Gaussian averaging associated with the diagonal disorder is discussed in detail in [1–3]. It depends on the variance, σ^2. Following [4–6], we carried out calculations for the square lattices with $\sigma = 0.263$, 0.186, 0.131, 0.093, and 0.066, where σ is in units of the ideal band width. Our results for the normalized optical absorption, $F(E)$, and the normalized density of states, $\rho(E)$, for the square lattice are shown in Figures 1 and 2, respectively. They are seen to be in good agreement with the finite-array calculations of Schreiber and Toyozawa as displayed in Figure 2 in [5] (absorption) and Figure 5(b) in [6] (density of states). This result is also consistent with [7], where a similar level of agreement was established for $E < -0.5$.

3. Rectangular Lattice

In the absence of disorder, the exciton energy for a rectangular lattice with unit band width takes the form

$$E_{\mathbf{k}} = -\frac{\left(\lambda \cos k_x + \cos k_y\right)}{2(\lambda + 1)}, \tag{3}$$

where λ is the interaction between neighboring sites on the x-axis. The corresponding expression for Green's function for complex energy is given in the Appendix to [8]

$$G_0(E) = 2(\lambda + 1)\left(\pi\lambda^{1/2}\right)^{-1} k_1(E)\,\mathbf{K}\left(k_1(E)\right), \tag{4}$$

where

$$k_1(E) = \left\{\frac{4\lambda}{\left[4(\lambda + 1)^2 E^2 - (\lambda - 1)^2\right]}\right\}^{1/2}. \tag{5}$$

Since the absorption is weakly affected by changes in λ, we focus on results for the density of states where we take $\sigma = 0.131$ and $\lambda = 0.5$, 1.0, and 1.5 (Figure 3). It is apparent that the density of states near the center of the band is strongly affected by changes in λ. The lower curve shows the results for $\lambda = 0.5$, the middle curve for $\lambda = 1.5$, and the upper curve for $\lambda = 1.0$. The dip at the center of the band, which grows stronger as with increasing anisotropy, reflects the fact that, in the limits $\lambda \gg 1$ and $\lambda \to 0$, the system approaches an array of decoupled chains with the consequence that the optical properties and the density of states become characteristic of one-dimensional arrays [1, 2].

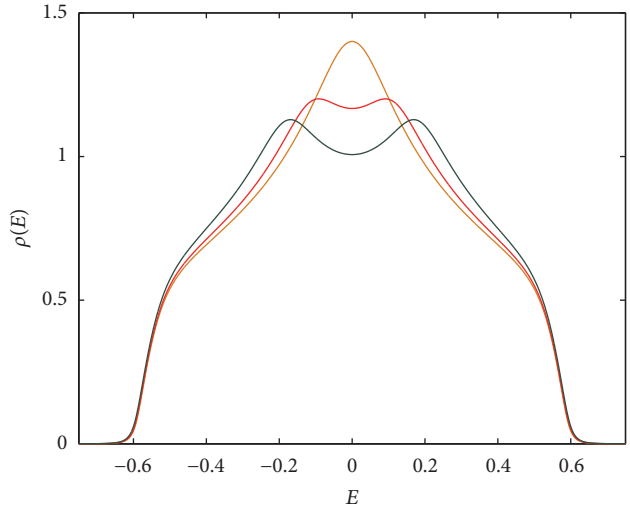

FIGURE 3: Normalized density of states for the rectangular lattice with $\sigma = 0.131$. From bottom to top at $E = 0$, the curves are for $\lambda = 0.5$, 1.5, and 1.0.

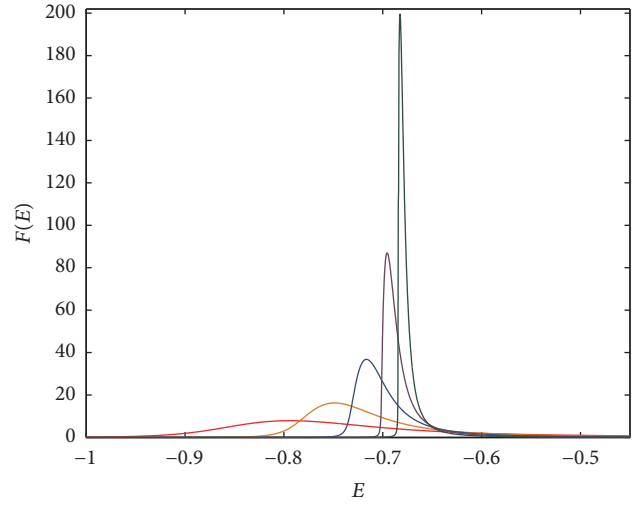

FIGURE 4: Normalized optical absorption for the triangular lattice. From left to right along the energy axis, the curves correspond to $\sigma = 0.263$, 0.186, 0.131, 0.093, and 0.066.

4. Triangular Lattice

In the absence of disorder, the exciton energy for the triangular lattice with unit band width has the form [9]

$$E_{\mathbf{k}} = -\left(\frac{2}{9}\right)\left(\cos 2k_x + 2\cos k_x \cos k_y\right) \tag{6}$$

with the optical absorption edge at −2/3 and the upper edge at 1/3. Analogous to the face-centered cubic lattice and unlike the square and rectangular lattices, the exciton band does not have a reflection point for the density of states. In units of the band width, the corresponding Green function for complex energy with negative real part has the form

$$G_0(E) = \left(\frac{9}{4\pi}\right) g(E)\, \mathbf{K}\left(k_2(E)\right), \tag{7}$$

where

$$g(E) = -\frac{8}{\left[(-9E+3)^{1/2}-1\right]^{3/2}\left[(-9E+3)^{1/2}+3\right]^{1/2}},$$
$$k_2(E) = \frac{4(-9E+3)^{1/4}}{\left[(-9E+3)^{1/2}-1\right]^{3/2}\left[(-9E+3)^{1/2}+3\right]^{1/2}}. \tag{8}$$

The results for the optical absorption and the density of states are shown in Figures 4 and 5, respectively. For small disorder, the absorption peaks are near the ideal (no disorder) band edge at −2/3. With increasing disorder, the absorption peak broadens and shifts to lower energy as occurs with the other lattices. In the case of the density of states, the ideal lattice has band edges at $E = -2/3$ and 1/3 as well as a singularity at $E = 2/9$. The behavior of the density of states below the absorption edge is shown in greater detail in Figure 6. It is similar to the corresponding results for the square lattice shown in [6, 7].

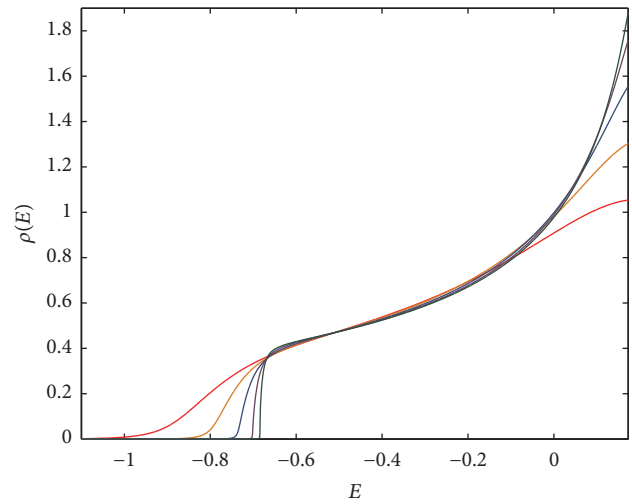

FIGURE 5: Normalized density of states for the triangular lattice. From left to right along the energy axis, the curves correspond to $\sigma = 0.263$, 0.186, 0.131, 0.093, and 0.066.

5. Anisotropic Triangular Lattice

For the triangular lattice discussed above all nearest-neighbor interactions are the same. In [10], Horiguchi investigated an anisotropic triangular lattice in which interactions along two of the three connecting lines took on the value γ while the interaction on the third line was equal to 1. When the optical edge is at the bottom of the band, the exciton energy is given by

$$E_{\mathbf{k}} = -\left[\cos(2ak_x) + 2\gamma\cos(ak_x)\cos\left(bk_y\right)\right], \tag{9}$$

where $a = 1/2$ and $b = \sqrt{3}/2$ when the length of the side of the triangle is 1 [10]. The lower and upper band edges and the band width (BW) are given in Table 1.

Table 1: The locations of the band edges and the band width for the ideal anisotropic triangular lattice. The nearest-neighbor interaction on two of the three lines of sites is equal to γ while it is equal to 1 on the third line [10].

Range of γ	Lower band edge	Upper band edge	Band width (BW)
$0 < \gamma < 2$	$-(1 + 2\gamma)$	$1 + \gamma^2/2$	$2 + 2\gamma + \gamma^2/2$
$\gamma = 2$	-5	3	8
$\gamma > 2$	$-(1 + 2\gamma)$	$2\gamma - 1$	4γ

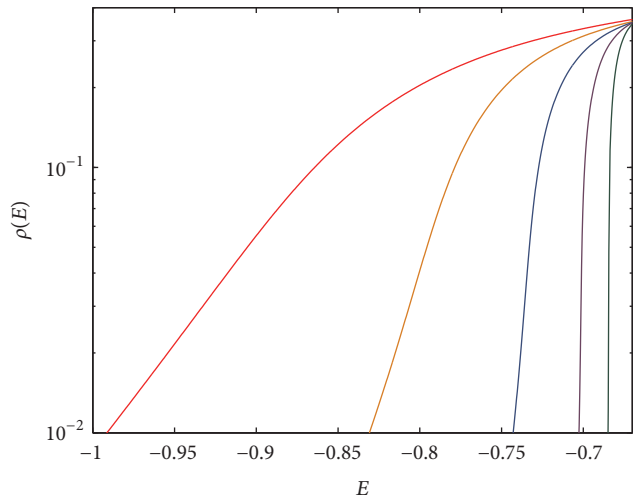

Figure 6: Semilog plot of the density of states below the absorption edge for the triangular lattice. From left to right along the energy axis, the curves correspond to σ = 0.263, 0.186, 0.131, 0.093, and 0.066.

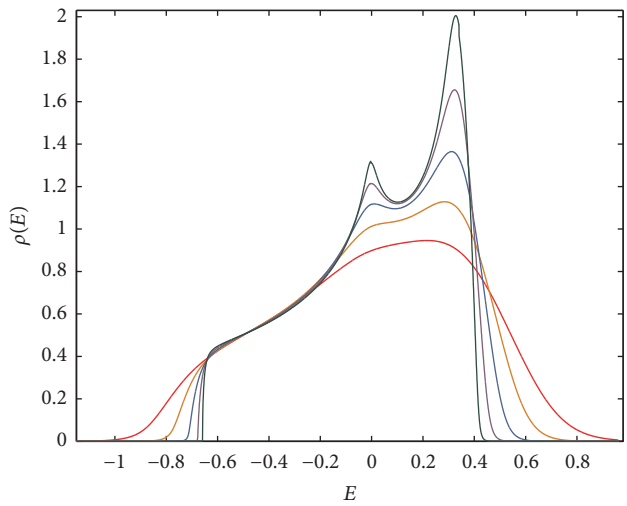

Figure 7: Normalized density of states for the anisotropic triangular lattice with $\gamma = 1/2$. From left to right along the energy axis, the curves correspond to σ = 0.263, 0.186, 0.131, 0.093, and 0.066.

The density of states is strongly affected by the ratio of the interaction strength. Apart from the band edges, the singularities in the ideal Green function for the anisotropic triangular lattice are associated with γ-dependent critical points on the energy axis and corresponding peaks in the density of states [10]. In units of the band width, BW, the peaks are at $(2\gamma - 1)$/BW and 1/BW for $0 < \gamma < 1$. For $\gamma = 1$, there is a single peak at 1/BW = 2/9. For $1 < \gamma < 2$, the peaks are also at $(2\gamma - 1)$/BW and 1/BW, and when $\gamma \geq 2$ there is a single peak at 1/BW. In Figure 7, we show the effects of disorder on the density of states for $\gamma = 1/2$. In this calculation, we made use of the expression for the Green function given in [10]. In the absence of disorder, the band edges are at −4/7 and 3/7, and the peaks are at 0 and 2/7.

6. Conclusions

The results for the square lattice extend the earlier work [7] to the entire spectrum. As we mentioned previously, our findings are consistent with numerical studies of the square lattice [5, 6]. The results for the rectangular arrays are expected to be reasonably accurate since the coherent potential approximation works well in the limiting cases $\lambda \gg 1$ and $\lambda \to 0$, where the rectangular array reduces to decoupled chains. In the case of the triangular lattice, finite-array calculations are needed to test the accuracy of the coherent potential approximation. If this is established, one has confidence that the approximation works reasonably well for the anisotropic triangular lattice since, in the limit $\gamma = 0$, the system decouples into independent chains, whereas when $\gamma \gg 1$, each site is strongly coupled to four nearest neighbors with the consequence that the behavior approaches that of the square array.

In the field of optical spectroscopy, a two-parameter assessment of the characteristics of the absorption line is provided by the peak position (E_{Peak}) and the full width at half maximum (FWHM). In Figure 8 we show the behavior of the two parameters with the increasing σ for both the square and triangular lattices. It is evident that the peak positions for the two lattices approach a common value for large σ whereas the increase in the linewidth occurs more rapidly for the square lattice. The latter behavior may reflect the fact that the effects of the disorder in the triangular lattice may be weaker due to an averaging of the contributions from a larger number of nearest neighbors.

Our results along with earlier studies [6, 7] suggest that the coherent potential approximation can be useful in interpreting the optical properties of two-dimensional systems with dominant nearest-neighbor interactions and Gaussian diagonal disorder provided the optically active states are Frenkel excitons. The findings reported in this paper are applicable to optically active monolayers. In addition,

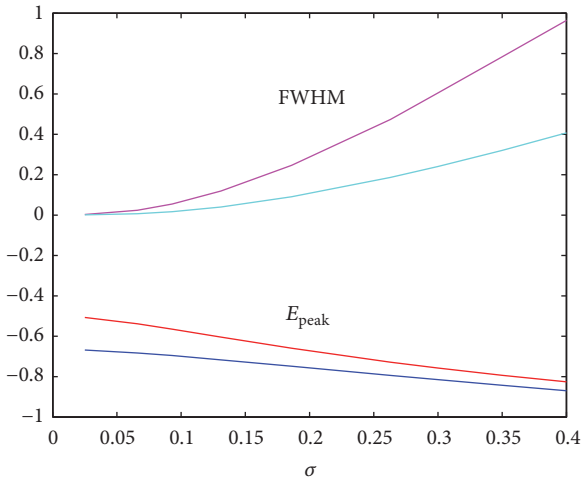

FIGURE 8: Peak position (E_{Peak}) and full width at half maximum (FWHM) versus σ for the square and triangular lattices. Energy and σ are in units of the band width. From top to bottom, square FWHM, triangle FWHM, square E_{Peak}, and triangle E_{Peak}.

there are quasi-two-dimensional magnetic exciton systems where the nearest-neighbor approximation is appropriate.

Conflicts of Interest

The authors declare that there are no conflicts of interest regarding the publication of this paper.

References

[1] I. Avgin, A. Boukahil, and D. L. Huber, "Accuracy of the coherent potential approximation for a one-dimensional Frenkel exciton system with a Gaussian distribution of fluctuations in the optical transition frequency," *Physica E: Low-Dimensional Systems and Nanostructures*, vol. 42, no. 9, pp. 2331–2334, 2010.

[2] A. Boukahil, I. Avgin, and D. L. Huber, "Assessment of the coherent potential approximation for the absorption spectra of a one-dimensional Frenkel exciton system with a Gaussian distribution of fluctuations in the optical transition frequency," *Physica E: Low-Dimensional Systems and Nanostructures*, vol. 65, pp. 141–143, 2015.

[3] I. Avgin, A. Boukahil, and D. L. Huber, "Coherent potential approximation for the absorption spectra and the densities of states of cubic Frenkel exciton systems with Gaussian diagonal disorder," *Physica B: Condensed Matter*, vol. 477, pp. 83–86, 2015.

[4] M. Schreiber, "Exciton absorption tails in one-dimensional systems," *Physical Review B*, vol. 34, no. 4, pp. 2914–2916, 1986.

[5] M. Schreiber and Y. Toyozawa, "Lineshape of the Exciton under Lattice Vibrations. III. The Urbach Rule," *Journal of the Physical Society of Japan*, vol. 51, no. 5, pp. 1544–1550, 1982.

[6] M. Schreiber and Y. Toyozawa, "Numerical Experiments on the Absorption Lineshape of the Exciton Under Lattice Vibrations. IV. The Indirect Edge," *Journal of the Physical Society of Japan*, vol. 52, no. 1, pp. 318–326, 1983.

[7] A. Boukahil and D. L. Huber, "Coherent potential approximation for the absorption spectra of a two-dimensional Frenkel exciton system with Gaussian diagonal disorder," *Modern Physics Letters B*, vol. 28, no. 32, Article ID 1450251, 2014.

[8] T. Morita and T. Horiguchi, "Calculation of the lattice green's function for the bcc, fcc, and rectangular lattices," *Journal of Mathematical Physics*, vol. 12, pp. 986–992, 1971.

[9] T. Horiguchi, "Lattice Green's functions for the triangular and honeycomb lattices," *Journal of Mathematical Physics*, vol. 13, pp. 1411–1419, 1972.

[10] T. Horiguchi, "Lattice Green's function for anisotropic triangular lattice," *Physica A. Statistical and Theoretical Physics*, vol. 178, no. 2, pp. 351–363, 1991.